

Hydraulic erosion of cohesive riverbanks

Jason P. Julian^{*}, Raymond Torres

Department of Geological Sciences, University of South Carolina, Columbia, SC 29208, U.S.A.

Received 6 May 2005; received in revised form 11 November 2005; accepted 14 November 2005

Available online 28 December 2005

Abstract

This study identifies and assesses the controls on hydraulic erosion of cohesive riverbanks on a 600-m reach of an urban ephemeral stream with active bank erosion. We examined hydraulic bank erosion by separating estimated bank shear stress into four properties: magnitude, duration, event peak, and variability. The values of these independent variables were used as a bank erosion context at three transects. Stepwise regression showed that the event peak (maximum peak) of excess shear stress best predicts cohesive bank erosion at the two transects with moderate critical shear stresses (1.93–4.08 N/m²), while the variability (all peaks) of excess shear stress best predicts erosion at the transect with low critical shear stress (0.95 N/m²). These results suggest that the amount of hydraulic erosion of cohesive riverbanks is dictated by flow peak intensities. Finally, the results of this study were combined with results from previous bank erosion studies to produce a conceptual model for estimating bank erosion rates based on their silt–clay content.

© 2005 Elsevier B.V. All rights reserved.

Keywords: River bank erosion; Process dominance; Magnitude–duration–intensity; Flow variability; Cohesive sediment transport; Channel evolution

1. Introduction

Identifying controls on cohesive riverbank erosion is a fundamental problem in fluvial geomorphology and hydraulic engineering. While noncohesive sediment is eroded through discrete particle entrainment that can be quantified using the magnitude of shear stress and particle size (Shields, 1936; Buffington and Montgomery, 1997), cohesive sediment is eroded through entrainment of aggregates (ASCE, 1968; Thorne, 1982). The electrochemical forces within and between aggregates cause their erosion to be complex (Grissinger, 1982; Le Bissonais, 1996;

ASCE, 1998; Simon and Collison, 2001). The detachment and subsequent entrainment of cohesive bank material can result from two processes: (i) hydraulic erosion—the lift and drag imposed by channel flow; or (ii) subaerial erosion—the weakening and weathering of bank material imposed by dynamic soil moisture conditions (Thorne, 1982; ASCE, 1998). In attempts to understand the complex nature of cohesive riverbank erosion, numerous studies have examined subaerial erosion (e.g., Twidale, 1964; Walker and Arnborg, 1966; Lawler, 1993; Rinaldi and Casagli, 1999; Prosser et al., 2000; Couper, 2003), and a few studies have investigated subaerial and hydraulic erosion collectively (e.g., Wolman, 1959; Knighton, 1973; Hooke, 1979). However, no study has been able to establish the predominant control on the amount of hydraulic erosion in response to variable flow conditions.

^{*} Corresponding author. Present address: Department of Geography, University of North Carolina, Chapel Hill, NC 27599-3220, U.S.A. Fax: +1 919 962 1537.

E-mail address: jjulian@unc.edu (J.P. Julian).

The lack of a strong correlation between flow conditions and hydraulic erosion is primarily due to the typical presence of subaerial erosion in cohesive riverbanks, which prevents an independent analysis of hydraulic erosion (Thorne, 1982; Simon et al., 2000). Cohesive riverbanks are usually poorly drained due to their silt and clay composition and thus may experience excess pore water pressures, one of the main agents of subaerial erosion (Thorne, 1982; Casagli et al., 1999). Clayey banks are also susceptible to desiccation cracking and slaking from wetting–drying cycles (Thorne, 1982), as well as freeze and thaw (Walker and Arnborg, 1966; Lawler, 1986, 1993; Gatto, 1995). The most successful attempts at independently analyzing hydraulic erosion have been through flume experiments in the laboratory (Arulanandan et al., 1980) and in situ (Grissinger et al., 1981). Arulanandan et al. (1980) found that erosion rates increased exponentially with decreasing soil resistance (i.e., critical shear stress), while Grissinger et al. (1981) found that erosion rates increased linearly with decreasing soil resistance. However, the force–resistance relationships in these flume experiments likely do not replicate field conditions (Arulanandan et al., 1980; Thorne, 1982; Couper, 2003). Force–resistance relationships are complicated in most natural channels as well due to fluctuating water tables (Casagli et al., 1999), seasonal vegetation (Thorne, 1990), active floodplain processes (Babaeyan-Koopaei et al., 2002), and the effects of previous flow events (Hooke, 1979). These force–resistance complications and the presence of subaerial erosion have impeded the identification of controls on hydraulic erosion of cohesive riverbanks.

The model most commonly used to predict hydraulic erosion rates of cohesive riverbanks (e.g., Osman and Thorne, 1988; Darby and Thorne, 1996; Langendoen and Simon, 2000) is:

$$E = k(\tau - \tau_c) \quad (1)$$

where E is lateral erosion rate, k is an erodibility coefficient, τ is applied shear stress by flow, and τ_c is critical shear stress for entrainment. This equation, which was developed from the flume study of Arulanandan et al. (1980), assumes that the amount of hydraulic erosion is a function of the magnitude (i.e., total amount) of excess shear stress ($\tau - \tau_c$). However, field studies have found other flow properties to be more strongly correlated to hydraulic erosion. For example, Wolman (1959) found that maximum bank erosion occurred during winter months. Winter storms, while not as intense as summer storms, were longer in dura-

tion thereby allowing flows to wear away thoroughly wetted banks. Wolman thus concluded that moderate, long duration storm-flow events cause the most erosion rather than high, short duration flows. Knighton (1973) found similar results as Wolman (1959), but added that flow variability (number of discharge peaks) also affects bank erosion. Knighton inferred that in addition to their longer durations, winter storm-flow events caused a much greater amount of erosion because of their multiple peaks as compared to summer storm-flow events which had single peaks. Although Wolman (1959) and Knighton (1973) acknowledged the occurrence of subaerial processes, including freeze–thaw, their research introduced the possibility that discharge duration and variability affect hydraulic erosion rates. Later, Hooke (1979) showed that at sites where hydraulic processes were dominant over subaerial processes, the variable with the strongest correlation to bank erosion was event peak discharge. Despite the variance ($r^2 \approx 0.46$) in these correlations, Hooke's results presented yet another control on hydraulic erosion. From these four studies, four possible flow properties emerged as controls on hydraulic erosion rates of cohesive riverbanks: magnitude (Arulanandan et al., 1980), duration (Wolman, 1959; Knighton, 1973), event peak (Hooke, 1979), and variability (Knighton, 1973).

The purpose of this paper is to evaluate hydraulic erosion in an urbanized channel in order to determine which independent flow property best predicts hydraulic erosion of cohesive riverbanks. In this study, bank erosion was evaluated in the context of four flow properties: magnitude, duration, event peak, and variability. These flow properties were assessed through temporal excess shear stress distributions. Field conditions suggest that channel boundary resistance was relatively constant and subaerial erosion was negligible.

2. Study area

The study site is the ephemeral upper reach (Fig. 1) of the Sand River in the Hitchcock Woods, an 8-km² protected urban forest located on the SW edge of Aiken, SC (33.60°N, 81.68°W). Sand River is a first-order tributary in the Savannah River basin. The 4.76-km² drainage area of Sand River includes the central business district of Aiken, which receives ~1200 mm of rain per year and rarely has temperatures below freezing (SERCC, 2004). The channel begins at a 3.05-m diameter outfall pipe, which is fed by a network of stormwater drainpipes distributed

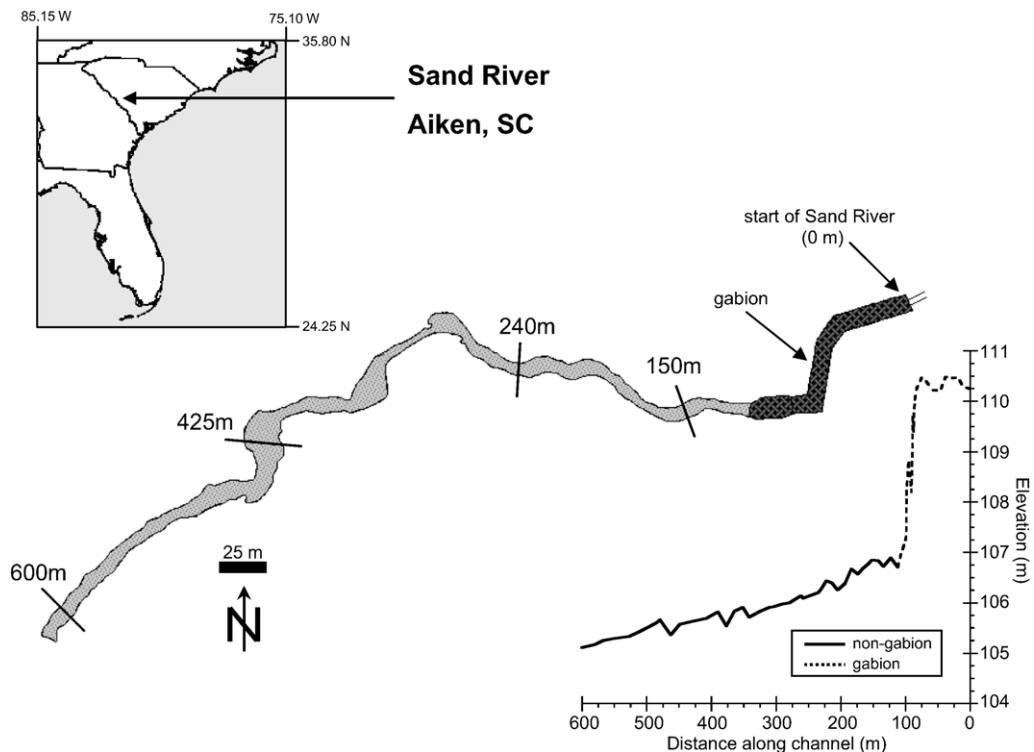


Fig. 1. Location of the transects monitored for bank erosion on Sand River. Distances on the longitudinal profile correspond to those on the channel map.

throughout the city limits. Four transects within the upper 600 m of Sand River (Fig. 1) were used for bank erosion analyses during the period of 6 December 2002–23 January 2004.

The Sand River meanders through a recently (c.a. 100 years) incised canyon composed of unconsolidated Late Cretaceous to Eocene fluvial and deltaic sediment (Nystrom et al., 1991). The channel is incised up to 25 m, and channel width ranges from 5 to 20 m. It is a sand-bed river with a slope of 0.0044 over its last 500 m of channel (Fig. 1). The first 100 m of channel bed and banks is a gabion (i.e., loose rock contained in a steel mesh), which dissipates flow energy before reaching the natural channel. Excluding the gabion, the channel banks are made up mostly of quartz sand with interstitial silt and clay throughout. The sand size is heterogeneous with no consistent pattern of fining upward or downward along the banks. At the four study sites, silt–clay contents range from 2.4% to 17.5%. The interstitial silt and clay cause the banks to be cohesive (Nystrom et al., 1991), as indicated by the vertical bank walls and the cohesive bank cores. Channel banks have been sporadically colonized by English ivy (*Hedera helix* L.) and Chinese privet (*Ligustrum sinense* Lour.). The

study reach is currently in its widening stage of channel evolution (see Schumm et al., 1984), as evidenced by the recurring bank erosion, lack of further entrenchment, and absence of a floodplain. In summary, Sand River is an ephemeral stream with cohesive banks that is widening in response to increased runoff from urbanization.

3. Methods

3.1. Erosion measurements

We assessed the cumulative effect of consecutive flow events on bank erosion at four transects (Fig. 2). The transects were surveyed five times each in approximately 3-month intervals, producing a total of four bank erosion measurements for each cross section. The datums we used for changes in width were the active channel widths (ACW) as described by Osterkamp and Hedman (1977) to be the upper limit of the channel that is being shaped by prevailing discharges. ACW was identified by a break in the steep bank slope to a more gently sloping surface and the lower limit of permanent vegetation (after Osterkamp and Hedman, 1977). Cross-sectional sur-

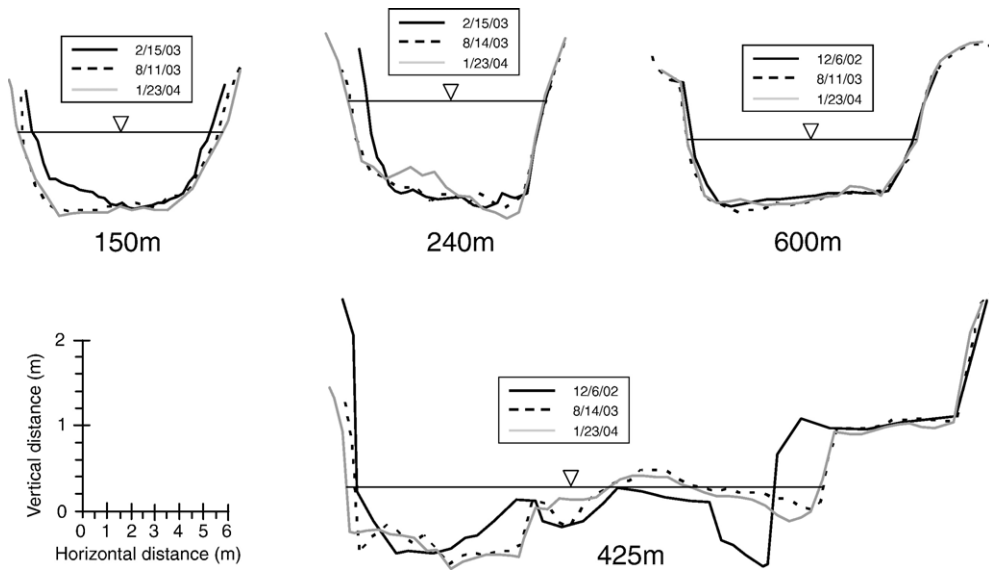


Fig. 2. Channel cross-sectional surveys at 150m, 240m, 425m, and 600m. The orientation of the surveys is left bank to right bank looking upstream. Resolution of measurements is 0.5 m for the bed and 0.25 m for the banks. Water surface denotes the active channel width (ACW) of the transect. (Note: For the purpose of clarity, intervening surveys are not shown.)

veys were also used to calculate flow depth–area relationships for the transects.

3.2. Flow measurements

Flow depth measurements were obtained with a *Starflow* hydrostatic pressure sensor (Model 6526-51, resolution=2.5 mm, error=± 6.25 mm) placed at the 150m transect from 6 December 2002 to 23 January 2004 (Fig. 3). We constructed a stage-discharge rating

curve (equation in Fig. 3) from in-stream discharge (Q) measurements using a *Marsh-McBirney* current meter (Model 2000). Flow depths (y), flow areas (A), and hydraulic radii (R) for 240m, 425m, and 600m were derived from the cross-sectional surveys in conjunction with Manning’s equation (Chow, 1959), using 150m as the reference transect and assuming equal Q . We assumed Q was uniform at each transect because there were no tributaries in the relatively short (600m) study reach. Although flow in Sand River was variable and

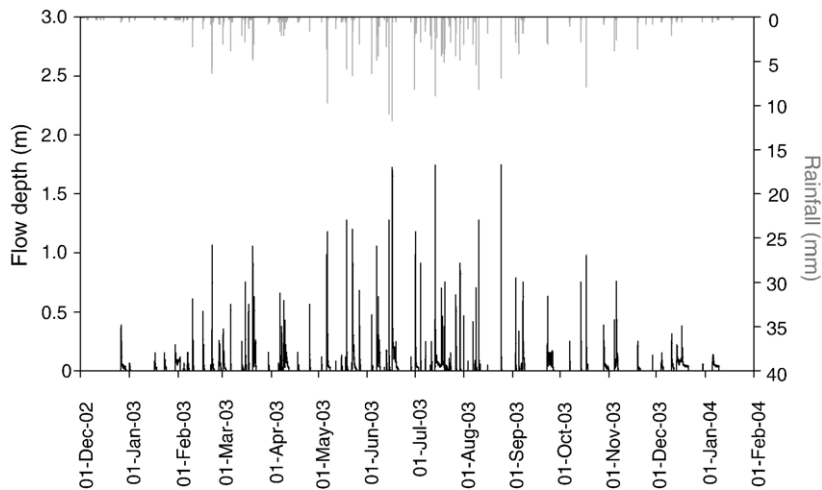


Fig. 3. Rainfall and flow depth at 150m (6 December 2002–23 January 2004). Resolution is 5-min. Discharge (Q) can be calculated from flow depth (y) using the following equation: $Q=8.17 * y^{2.01}$.

had a high suspended sediment load, the Manning’s approach was applicable because (i) channel slope was low ($S=0.0044$), with minimal variations (Fig. 1); (ii) bed roughness was small ($D_{50}=0.35$ mm) and relatively uniform; and (iii) channel shape was approximately trapezoidal (Fig. 2). We calculated Manning’s roughness coefficient (n) for 150m from the stage-discharge rating curve. We used the Cowan (1956) method to estimate n for the other three transects as it takes into account the subtle variations between cross sections (i.e., surface irregularities, variations in channel cross-sectional size and shape, effect of obstructions, in-channel vegetation, and channel meandering). Because we only had a stage-discharge rating curve for 150m, we assumed that n decreased with increasing discharge for the other three transects at the same rate as 150m. Maximum n values at 150m, 240m, 425m, and 600m were 0.041, 0.050, 0.048, and 0.037, respectively.

Due to equipment malfunctions, 20 of the 74 total flow events (defined in Section 3.5) had to be modeled utilizing rainfall data from a gauge (5-min summations, resolution=0.254 mm) we placed in the center of the Sand River watershed. We modeled flow depths by using the hydrographs of storms with similar magnitude (total rain amount), duration (rain duration), variability (number of rain peaks above 1 mm), and intensity (30-min maximum rain total). The use of 30-min maximum intensity results from its strong correlation ($r^2=0.90$) to maximum flow depth. The concept of using similar storms to model flow events was based on the assumption that in a small urban watershed where temporal and spatial variability of rainfall is negligible, storms of the same magnitude, duration, variability, and intensity produce similar flow stages.

3.3. Applied shear stress

Applied bank shear stress (τ_{bank}), in N/m^2 , was calculated in 5-min intervals from the method of Flinham and Carling (1988):

$$\text{SF}_{\text{bank}} = 1.77 \left(\frac{P_{\text{bed}}}{P_{\text{bank}}} + 1.5 \right)^{-1.4} \tag{2}$$

$$\tau_{\text{bank}} = \tau * \text{SF}_{\text{bank}} \left(\frac{B + P_{\text{bed}}}{2 * P_{\text{bank}}} \right) \tag{3}$$

where SF_{bank} is the proportion of the total cross-sectional shear force acting on the bank, P_{bed} and P_{bank} are the wetted perimeters of the bed and banks, respectively, B is the water surface width, and τ is the cross-sectional shear stress. Data from other studies support this approach (e.g., ASCE, 1998). Channel cross-sectional shear stress, which is the time-averaged force of water per unit area of the channel boundary, was calculated using the following equation (Chow, 1959):

$$\tau = \gamma RS \tag{4}$$

where γ is the specific weight of water (9800 N/m^3) and S is the energy slope. We calculated R by dividing A by P , which were found using the cross-sectional surveys in combination with in-channel flow measurements.

3.4. Critical shear stress

We estimated critical shear stress (τ_c) by using silt-clay (<0.063 mm) percentage ($SC\%$) as a predictor (after Vanoni, 1977) combined with observations by Dunn (1959). We applied a third-order polynomial

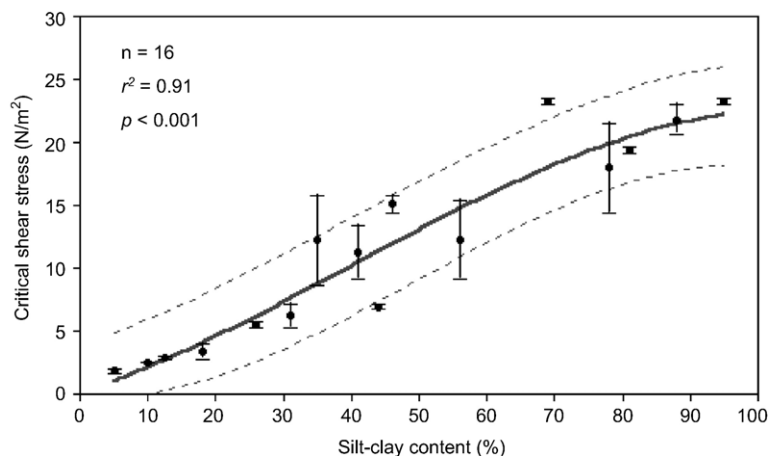


Fig. 4. Critical shear stress estimate from silt-clay percentage (data from Dunn, 1959). Each point represents the average critical shear stress for a soil sample with a specified silt-clay percentage. The average value was derived from 2 to 4 tests on each soil sample. Error bars represent the maximum and minimum values of the tests for each soil sample. The dashed lines are 95% confidence intervals for the rating curve.

Table 1
Critical shear stress coefficients to account for vegetation

Bank vegetation	τ_c coeff
None	1.00
Grassy	1.97
Sparse trees	5.40
Dense trees	19.20

trend line to Dunn's average values of τ_c in order to generate a rating curve for τ_c based on $SC\%$ (Fig. 4). We used a third-order polynomial based on the assumption that at 100% silt–clay, τ_c would reach a maximum value, and at 0% silt–clay, τ_c would reach a minimum value. The trend line was forced through the y -axis (0% silt–clay) at 0.1 N/m^2 , which is the lower limit of the Shield's curve (Shields, 1936). From this procedure, we generated the following rating curve:

$$\tau_c = 0.1 + 0.1779(SC\%) + 0.0028(SC\%)^2 - 2.34E - 5(SC\%)^3. \quad (5)$$

Reported τ_c values from other bank erosion studies support this relation (Papanicolaou, 2001; Gaskin et al., 2003; Simon et al., 2003). How τ_c varies with time and flow conditions has not been established (ASCE, 1998) and consequently was not incorporated into the rating curve. We obtained $SC\%$ of the channel banks through four bank cores (depth=5 cm, volume=90.5 cm³) at each transect.

Vegetation likely increases τ_c of channel banks (Thorne, 1990; ASCE, 1998). Therefore, we used vegetation coefficients (i.e., multiplication factors) in conjunction with τ_c values from Eq. (5). We obtained these coefficients (Table 1) from the data of Huang and Warner (1995) and Huang and Nanson (1998), who derived bank strength indices for various bank types with different levels of vegetation cover and related them to τ_c . Millar and Quick (1998) reported similar coefficients for τ_c between different bank vegetation types. For channel banks in Sand River with Chinese privet (*L. sinense* Lour.), we used τ_c coeff for “sparse” and “dense” trees (Table 1). For channel banks with English ivy (*H. helix* L.), we adapted τ_c coeff from “grassy” (Table 2) on the basis that both have small, shallow roots and dense ground cover. The slight differences between the two types of vegetation (i.e., ivy having stems, larger leaves, and more variable surface densities) were taken into account in Table 2.

3.5. Excess shear stress

Temporal distributions of excess shear stress (τ_{ex}) were calculated for all flow events of each transect

individually by subtracting the τ_c values from the τ_{bank} values ($\tau_{ex} = \tau_{bank} - \tau_c$). Any negative values, where τ_c was greater than τ_{bank} , were modeled to be zero since τ_c represents a threshold that must be exceeded in order to have τ_{ex} . A flow event for this ephemeral stream was defined as any flow in the channel above 1 cm depth. A flow event therefore could have multiple peaks as long as the flow depth remained above 1 cm. Evaluating τ_{ex} distributions on this flow event basis provided a bank erosion context in which the following properties were used as independent variables (Fig. 5):

- I. Magnitude (N/m^2), $\sum(\tau_{bank} - \tau_c)$
- II. Duration (min), $\text{time}_{(\tau_{bank} > \tau_c)}$
- III. Event peak (N/m^2), $(\tau_{bank} - \tau_c)_{max}$
- IV. Variability (N/m^2), $\sum(\tau_{bank} - \tau_c)_{peaks}$.

The values of these four τ_{ex} properties were assessed individually for each erosion measurement interval in order to determine the cumulative effect of each property on the measured erosion values.

3.6. Statistical methods

Stepwise regression was used to find which property (I–IV) had the strongest relationship to bank erosion. This method used an analysis of variance model to search through all independent variables (τ_{ex} properties) and determine which one had the strongest correlation to the dependent variable (bank erosion). The level of significance is 90% ($\alpha=0.10$), which Draper and Smith (1998) found to be conservative enough to include all potential explanatory variables yet constrained enough to extract the true explanatory variable. F -statistics ($df_{model}=1$, $df_{error}=n-2$) and p -values provided the basis to test the null hypothesis that the dependent variable is not linearly related to the independent variable. Stepwise regression was performed on each transect separately using SAS statistical software.

Spearman's rho (ρ), a nonparametric test, was used to address the limitation of stepwise regression not taking into account rank correlation (i.e., a greater

Table 2
Critical shear stress coefficients for ivy based on areal coverage

Areal coverage	τ_c coeff
None (0%)	1.0
Sparse (<25%)	1.5
Medium (25–75%)	2.0
Dense (>75%)	2.5

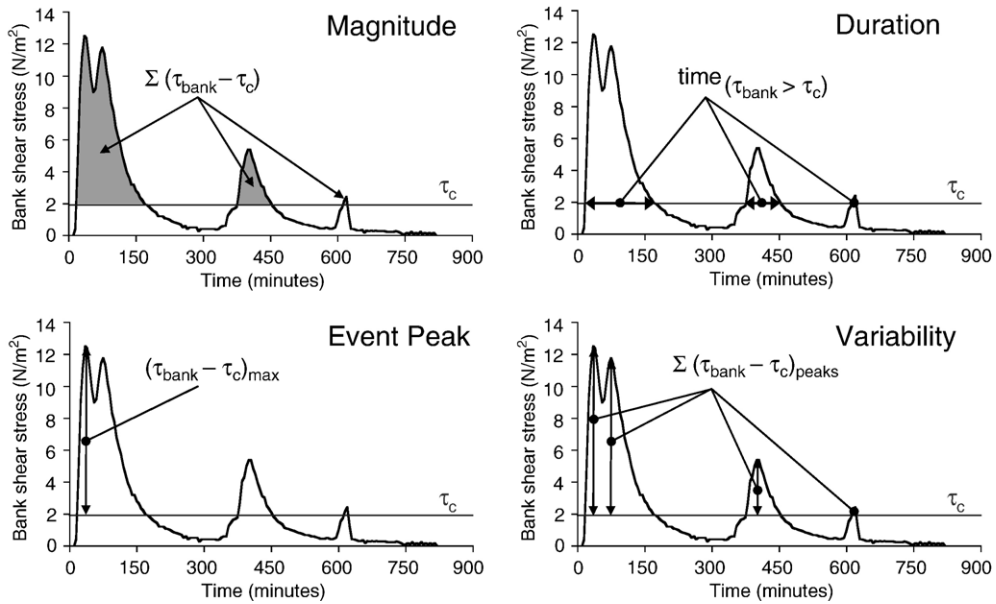


Fig. 5. Flow event properties of the excess shear stress distribution. Bank and critical shear stress values represent a flow event at 150m on 26 July 2003.

sum of force results in a greater amount of erosion), and assess the strength of the association between the independent and dependent variables. This approach takes into consideration the ranks of the data rather than the nominal values. A value of $\rho = 1.0$ indicates perfect rank correlation between the independent (X) and dependent variable (Y). We used ρ to test the null hypothesis that X_i and Y_i are mutually independent. In order to reject the null hypothesis at the 95% significance level ($\alpha = 0.05$) and infer dependence, ρ for this sample size ($n = 4$) had to be greater than 0.80 (Conover, 1999). Rho values, calculated using SAS, were used to either confirm or reject the results of stepwise regression.

4. Results

4.1. Rainfall and runoff

There were 74 storms (i.e., rainfall coinciding with flow event) from 6 December 2002 to 23 January 2004 (Fig. 3), supplying a precipitation total of 1550 mm to the Sand River watershed. Summer storms were characterized by high intensities, producing the eight most intense (30-min maximum) storms. The average response time for Sand River (i.e., the time difference between the start of rainfall and the start of streamflow) was $29 \text{ min} \pm 12$. The maximum proportion of rainfall that resulted in runoff was 0.57. When there was no flow in the channel, we measured the water table to be 30–50

cm below the bed surface. Discharges ranged from 0 to $25 \text{ m}^3/\text{s}$. The maximum discharge of $25 \text{ m}^3/\text{s}$, which is set by the stormwater drainpipes, occurred three times during our study (Fig. 3). Sediment from unpaved roads and footpaths caused runoff into Sand River to be laden with fine sediment, thus preventing the effect of “hungry water” (Kondolf, 1997) on bank erosion.

4.2. Bank erosion

Over the 14-month study, $\sim 2800 \text{ m}^3$ of bank material was eroded from the upper 600 m of Sand River. Cross-sectional surveys of the analyzed transects are displayed in Fig. 2. All channel widening at the four transects was observed to be the result of hydraulic erosion. Bank failures occurred in the channel, but were the direct result of hydraulic undercutting. None of the transects contained major in-channel debris (e.g., trees, boulders), thereby eliminating local scour effects. The temporal variability in bed geometries is due to the sensitivity of sand-bed streams to floods and sediment supply. Bank erosion occurred on both banks of the 150m and 425m transects and on the left bank of the 240m transect. The right bank of 240m and the right bank of 600m did not experience erosion. The left bank of 600m experienced erosion during only one measurement interval. Consequently, 600m was not used in any statistical analyses because its data distribution (three zero values and one non-zero value) produced biased correlations. The result of this exclusion is that there

were three sets of bank erosion measurements available for statistical analyses, the 150m, 240m, and 425m transects. During the study period, ACW increased at all four transects: 1.09 m at 150m, 0.76 m at 240m, 2.51 m at 425m, and 0.15 m at 600m (Fig. 2).

4.3. Bank resistance

Silt–clay contents of the four transects varied from 2.8% to 12.4% (Table 3). The amount of silt–clay content variability within each transect was not large, either between upper and lower bank or between left and right bank. The average difference between upper and lower bank of the same transect was $4.7\% \pm 2.6$. The average difference between left and right bank of the same transect was $3.4\% \pm 2.4$. This low bank composition variability within transects minimized the error associated with assigning one average τ_c for each transect. Two of the transects (240m and 600m) had vegetation on both of their banks, while the other two transects (150m and 425m) did not have vegetation on either of their banks (Table 3). Critical shear stresses ranged from 0.95 to 17.83 N/m² (Table 3). The relationship between τ_c and bank erosion rate at the four transects had a power trend ($r^2=0.98$, $p=0.012$) (Fig. 6). This exponential relationship was also found by Arulanandan et al. (1980).

4.4. Bank forces

Using Eq. (3), τ_{bank} at 150m reached a maximum of 0.76 τ . This maximum value of 0.76 for the portion of shear stress applied to banks of trapezoidal channels has also been reported by Chow (1959) and Chang (1988). Maximum τ_{bank} values at 240m, 425m, and 600m were slightly lower at 0.72, 0.73, and 0.71 τ , respectively. These lower values of τ_{bank} were due to 240m, 425m, and 600m having higher $P_{\text{bed}}/P_{\text{bank}}$ values than 150m,

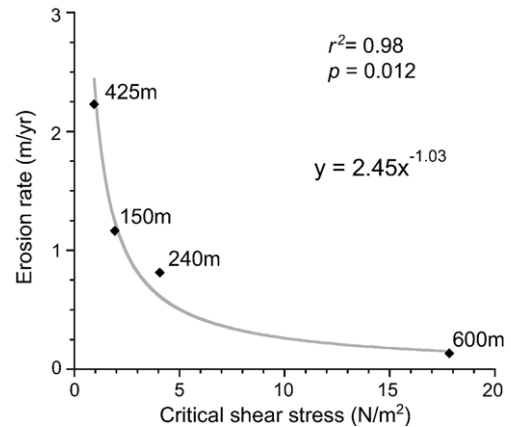


Fig. 6. Relation between bank erosion rates and bank resistance at Sand River over the 14-month study.

which is attributed to their geometries (Fig. 2) being farther along in the floodplain development process (see Schumm et al., 1984).

Of the 74 flow events, excess shear stresses occurred in 53 of the events at 150m, 44 at 240m, 59 at 425m, and 19 at 600m. Nonparametric one-way analysis of variance (ANOVA) established that there was not a significant ($\alpha=0.05$) difference of average event values between erosion measurement intervals for *magnitude*, *duration*, or *variability*. The average value of *event peak*, however, was found to be significantly different between erosion measurement intervals for 150m, 240m, and 600m. These ANOVA results indicate that the only τ_{ex} property that differed between seasons in Sand River was *event peak*. Multicollinearity did not exist for the property event values, which means that *magnitude*, *duration*, *event peak*, and *variability* were independent of one another on an event basis. Multicollinearity, however, did exist for the property summation values used for stepwise regression, which we attribute to the disparity of total storm runoff between measurement intervals. An interval of high runoff had

Table 3
Critical shear stresses for transects

Transect	Bank	Silt–clay content (%)	τ_c^* (N/m ²)	Vegetation/density	τ_c coeff	τ_c^{**} (N/m ²)	τ_c (N/m ²)
150m	Left	12.4	2.69	None	1.0	2.69	1.93
	Right	5.6	1.18	None	1.0	1.18	
240m	Left	8.2	1.73	Ivy/Sparse	1.5	2.60	4.08
	Right	10.4	2.22	Ivy/Dense	2.5	5.56	
425m	Left	2.8	0.62	None	1.0	0.62	0.95
	Right	6.1	1.28	None	1.0	1.28	
600m	Left	7.2	1.52	Privet/Dense	19.2	29.18	17.83
	Right	5.7	1.20	Privet/Sparse	5.4	6.48	

τ_c^* is the critical shear stress based solely on silt–clay percentage (Eq. (5)). τ_c coeff are the vegetation coefficients obtained from Tables 1 and 2. τ_c^{**} is the critical shear stress values taking into account the effects of vegetation, calculated by multiplying τ_c^* by τ_c coeff. τ_c is the average critical shear stress value for the transect, calculated by taking the average of the left and right banks.

high summation values for all four properties; whereas, an interval of low runoff had low summation values for all four properties. This multicollinearity only permits the results of stepwise regression to be used as the best predictor of hydraulic erosion (i.e., the cause of hydraulic erosion cannot be established).

4.5. Stepwise regression and rank correlation

Bank erosion was first compared to storms (the number of storms during the measurement interval

that had τ_{ex}) to investigate if bank erosion was merely the result of an τ_{ex} event (Fig. 7). The variable *storms* does not take into account any of the properties of magnitude, duration, event peak, or variability. So, if *bank erosion* was strongly correlated to *storms*, the assumption that a particular property of the τ_{ex} distribution controlled bank erosion would be negated. The association between these two variables was weaker than all other variables ($r^2=0.63, 0.56,$ and 0.74 for 150m, 240m, and 425m, respectively). Stepwise regression confirmed the weak correlation by not includ-

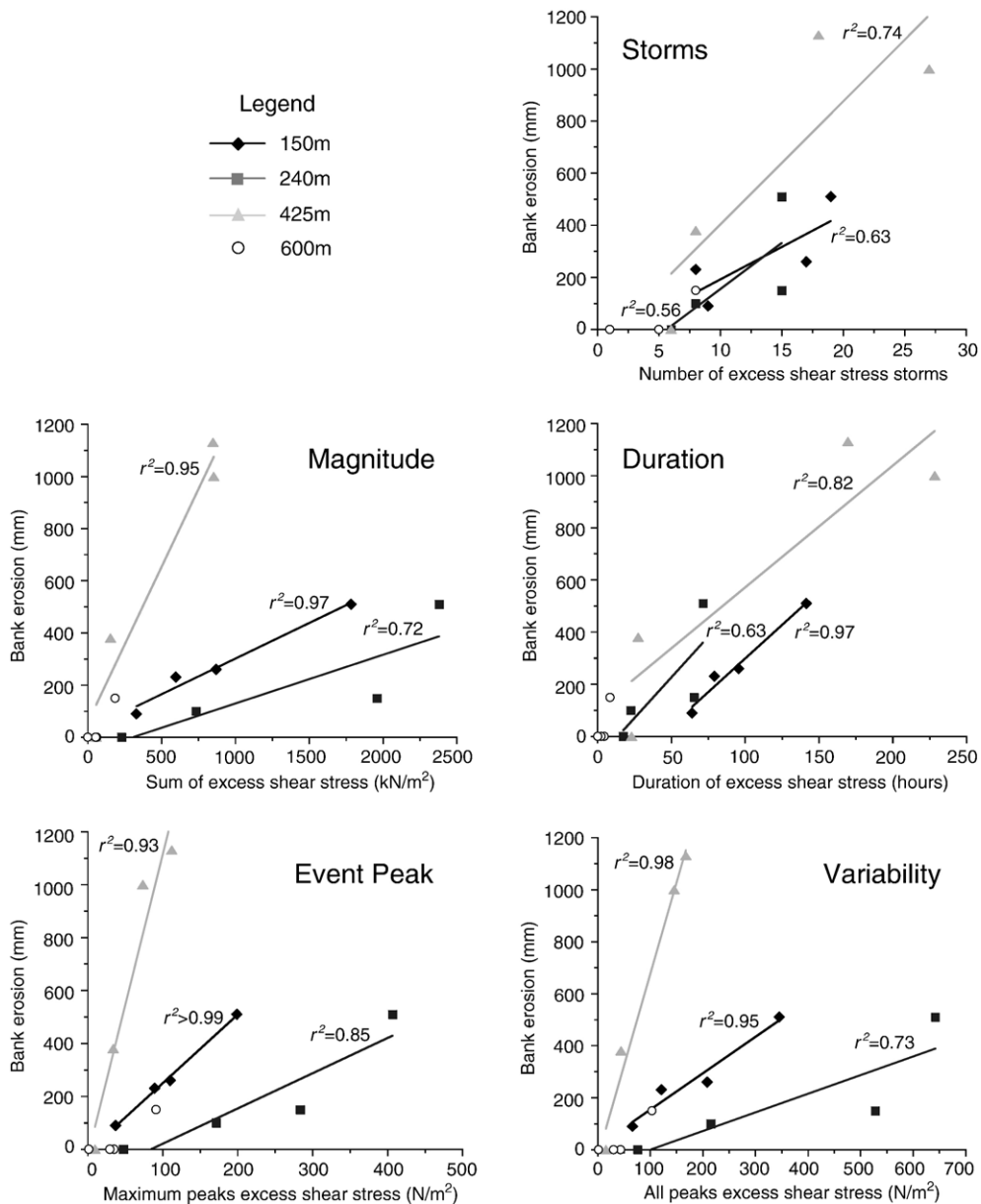


Fig. 7. Relations between bank erosion and flow event properties of the excess shear stress distribution.

ing *storms* as an explanatory variable (i.e., rank #1 and p -value <0.10) for any of the transects (Table 4). Spearman rank correlation substantiated the weak correlation with perfect rank correlation absent in all three transects (Table 4). The weak association between *bank erosion* and *storms* therefore does not invalidate the assumption that some property of the τ_{ex} distribution dictates the amount of hydraulic bank erosion.

Bank erosion vs. magnitude (Fig. 7) yielded r^2 values of 0.97, 0.72, and 0.95 for 150m, 240m, and 425m, respectively. The regression lines of the *magnitude* plot follow a logical pattern. As τ_c decreases from 240m (4.08 N/m²) to 150m (1.93 N/m²) to 425m (0.95 N/m²), the rate of bank erosion increases as shown by the increasing slopes of the regression lines. This pattern is expected since banks of lower resistance are more sensitive to bank erosion than banks of higher resistance. Despite the higher r^2 values and the logical pattern of regression lines, stepwise regression did not include *magnitude* as an explanatory variable for any of the transects and *magnitude* rank correlation was not present at 425m (Table 4).

Bank erosion vs. duration (Fig. 7) yielded r^2 values of 0.97, 0.63, and 0.82 for 150m, 240m, and 425m, respectively. The regression lines of this plot did not follow the same logical pattern as those of the *magnitude* plot. Accordingly, stepwise regression did not include *duration* as an explanatory variable for any of the transects and *duration* rank correlation was not present at 425m (Table 4).

Bank erosion vs. event peak (Fig. 7) yielded the highest r^2 values for 150m and 240m, >0.99 and 0.85, respectively. The r^2 value for 425m was 0.93.

Table 4
Stepwise regression and Spearman rank correlation for excess shear stress vs. bank erosion

Transect	Rank	Variable	r^2	F	p	ρ
150m	1	Event peak	0.996	509.74	0.002	1.00
	2	Duration	0.975	77.47	0.013	1.00
	3	Magnitude	0.974	75.61	0.013	1.00
	4	Variability	0.949	37.51	0.026	1.00
	5	Storms	0.632	3.43	0.205	0.80
240m	1	Event peak	0.849	11.22	0.079	1.00
	2	Variability	0.730	5.42	0.145	1.00
	3	Magnitude	0.724	5.24	0.149	1.00
	4	Duration	0.629	3.40	0.207	1.00
	5	Storms	0.560	2.54	0.252	0.95
425m	1	Variability	0.980	98.57	0.010	1.00
	2	Magnitude	0.948	36.23	0.026	0.80
	3	Event peak	0.933	27.74	0.034	1.00
	4	Duration	0.822	9.24	0.093	0.80
	5	Storms	0.746	5.86	0.136	0.80

Along with the *magnitude* plot, the regression lines followed the logical pattern of increasing erosion rates with decreasing τ_c . Stepwise regression found *event peak* to be the explanatory independent variable for *bank erosion* at 150m and 240m with “ F -, p -values” of “509.72, 0.002” and “11.22, 0.079,” respectively (Table 4). Spearman rank correlation confirmed the results of stepwise regression with perfect *event peak* rank correlation for all three transects (Table 4).

Bank erosion vs. variability (Fig. 7) yielded the highest r^2 value for 425m with 0.98. The r^2 values for 150m and 240m were 0.95 and 0.73, respectively. The regression lines of this plot also had the logical pattern of increasing erosion rates with decreasing τ_c . Stepwise regression found *variability* to be the explanatory independent variable for *bank erosion* at 425m with an F -value of 98.57 and a p -value of 0.010 (Table 4). Spearman rank correlation confirmed the results of stepwise regression, finding perfect *variability* rank correlation for all three transects (Table 4).

In summary, bank erosion rates between the four transects increased with decreasing τ_c . *Event peak* was found to be the explanatory variable for *bank erosion* at 150m and 240m, and *variability* was found to be the explanatory variable for *bank erosion* at 425m. *Magnitude* and *duration* were not found to be explanatory variables for hydraulic erosion at any of the transects.

5. Discussion

5.1. Excess shear stress as a bank erosion context

Results of this study indicate that there was an explanatory independent variable for bank erosion at the 90% significance level for all transects involved in the analyses. Although the results are derived from a small sample size, the strength of the correlations provides evidence that there is a link between certain properties of excess shear stress and hydraulic erosion of cohesive riverbanks. Event peak had the strongest correlation to bank erosion in the two transects with moderate τ_c (1.93–4.08 N/m²). In the transect with low τ_c (0.95 N/m²), variability had the strongest correlation to bank erosion. Though different properties, both are measures of intensity (i.e., magnitude of τ_{ex} at a particular time). The fact that banks with low τ_c are more strongly correlated to intensity of all peaks rather than just the highest peak of a flow event suggests that banks with low resistance are more susceptible to flow stage variability. These results indicate that the amount of hydraulic erosion of cohesive riverbanks is dictated by flow peak intensities.

Statistical analyses revealed that the strongest correlations were present at 150m, which we attribute to the flow gage at the transect and the absence of bank vegetation. The flow gage allowed us to use direct measurements of y and n for 150m. Having to use estimates of y and n for the other transects probably introduced error to their τ_{bank} calculations. Lower r^2 values for 240m were consistent in all regression plots. The most likely explanation is that the effect of vegetation on τ_c was underestimated. The effect of *H. helix* L. and *L. sinense* Lour. on τ_c has not been quantified, and thus our estimates of τ_c *coeff* probably have considerable error associated with them. The higher r^2 values at 425m, along with 150m, are attributed to not having to use a τ_c *coeff* for vegetation effects. A source of possible error in our τ_{bank} values was the use of Eq. (3), which was developed from artificial channels that did not possess in-channel vegetation or irregular geometries (Flintham and Carling, 1988). Both of these factors can reduce the force of flow on the channel perimeter (Thorne, 1990; Khodasheenas and Paquier, 1999). Eq. (3) therefore is susceptible to overestimates of τ_{bank} in natural channels. This probable error in τ_{bank} is believed to be partly responsible for the presence of zero values of bank erosion at 240m, 425m, and 600m despite having τ_{ex} . The exact values of τ_{ex} may be in error; however, their proportionality between properties was not affected as a consequence of using the same approach to derive all τ_{ex} values (Eqs. (2)–(5); Tables 1 and 2).

5.2. Discharge as a bank erosion context

We reevaluated bank erosion using Q as the independent variable to investigate how our results compare to an analysis that uses only direct measurements. The values of Q that we used in this analysis came from the flow gage (via the stage-discharge rating curve), and thus are not susceptible to the possible errors mentioned above. Stepwise regression and Spearman rank correlation of *bank erosion* vs. Q (Table 5) confirmed the results of our analysis using τ_{ex} (Table 4). Both analyses found *event peak* to be the explanatory variable at 150m and 240m, and *variability* to be the explanatory variable at 425m. The only variable that was consistently ranked different by the two analyses was *duration*. We ascribe this disparity to the fact that low discharges do not contribute to erosion, and therefore Q duration will not be strongly correlated to bank erosion. Despite the high r^2 of the explanatory variables in the Q analysis, we do not recommend using Q as a bank erosion context because it is not a direct measure of force. In addition to the lack of significance of low discharges, equal discharges

Table 5
Stepwise regression and Spearman rank correlation for discharge vs. bank erosion

Transect	Rank	Variable	r^2	F	p	ρ
150m	1	Event peak	0.998	961.73	0.001	1.00
	2	Variability	0.981	101.60	0.010	1.00
	3	Magnitude	0.878	14.42	0.063	0.80
	4	Storms	0.597	2.96	0.227	0.95
	5	Duration	0.185	0.45	0.570	0.80
240m	1	Event peak	0.916	21.84	0.043	1.00
	2	Variability	0.823	9.27	0.093	1.00
	3	Magnitude	0.764	6.47	0.126	0.80
	4	Storms	0.579	2.75	0.239	0.95
	5	Duration	0.057	0.12	0.762	0.60
425m	1	Variability	0.978	90.32	0.011	1.00
	2	Magnitude	0.899	17.82	0.052	0.80
	3	Event peak	0.889	15.95	0.057	1.00
	4	Storms	0.669	4.04	0.182	0.74
	5	Duration	0.298	0.85	0.454	0.60

will not always contribute to bank erosion equally. For example, in a river transect experiencing bank erosion, two discharges of the same magnitude will not produce the same shear stresses because, as the channel widens, the hydraulic radius will decrease, creating lower shear stresses (Simon, 1992).

5.3. Experimental design

We attribute the high correlations of the statistical analyses to the use of an ideal study site, and to the use of small temporal and spatial scales. In previous field studies on cohesive bank erosion (e.g., Wolman, 1959; Knighton, 1973), force–resistance relationships were complicated by the presence of confounding variables: fluctuating water tables, freeze–thaw, seasonal vegetation, active floodplains, and excess pore-water pressures. In this study, a field site was used that had the following characteristics: (i) an ephemeral stream where the water table was not high enough to wet the channel banks; (ii) well-drained banks (low silt–clay content) that minimized excess pore water pressures, desiccation cracking, and slaking; (iii) an entrenched channel that did not have an active floodplain; (iv) nonseasonal in-channel vegetation; and (v) located in a warm region in which freeze–thaw processes were negligible. These characteristics allowed us to reason that channel boundary resistance was relatively constant and the effects of subaerial erosion were minimized to the point where erosion could be considered as a direct consequence of hydraulic processes.

Erosion measurements were collected from a segment of 450 m over a period of 14 months. This relatively small spatial and temporal scale limited the

number of variables in the experiment and constrained the ones that were present. The small spatial scale prevented influences from tributaries (e.g., increased discharge, backwater effect) and major changes in channel geometry (e.g., active floodplain). Further, this study only compared erosion measurements to those of the same cross section, thereby eliminating the factor of variable channel geometries, velocity distributions, and bank compositions. The threshold for erosion was thus held relatively constant. The small temporal scale prevented changes in flow regime (e.g., land use change) and channel characteristics (e.g., vegetation invasion). Over larger spatial and temporal scales, these added variables would complicate force–resistance relationships and add a great deal of variance to the regression plots of bank erosion (see Benda et al., 2002). Additionally, in contrast to event-based erosion measurements, this study minimized the error associated with the effect of previous flow events (Hooke, 1979; Newson, 1980; Beven, 1981; Rhoads and Miller, 1991) by analyzing cumulative erosion over a series of flow events.

5.4. Cohesive bank erosion

Wolman (1959) found that the amount of cohesive bank erosion was dictated by flow duration. His study was conducted on channel banks with high *SC%* (45–80%), which means that subaerial processes were a factor. Therefore, the bank erosion measured by Wolman was probably not entirely the result of hydraulic shear. Knighton (1973), whose study site had low bank *SC%* (3–23%), found that the presence of multiple flow peaks was a factor in amount of erosion. Hooke (1979) found that the erosion of banks with higher *SC%* was more strongly correlated to bank moisture conditions, while the erosion of banks with lower *SC%* was more strongly correlated to flow conditions. Couper (2003) found that riverbanks with higher silt–clay contents were more susceptible to subaerial erosion than those with lower silt–clay contents.

The inferences of the above studies are combined with the results of this study to produce a conceptual model that identifies which independent flow variable best predicts erosion rates of riverbanks with a specified silt–clay content (Fig. 8). Erosion of channel banks with high *SC%* (>40%) is dominated by subaerial processes. These processes include leaching, desiccation, slaking, piping, freeze–thaw, and mass failure (Thorne, 1982). Because all of these processes are directed by soil moisture conditions, duration of τ_{ex} is the best predictor of bank erosion rates. In banks with high *SC%*, the amount of erosion from hydraulic shear is usually neg-

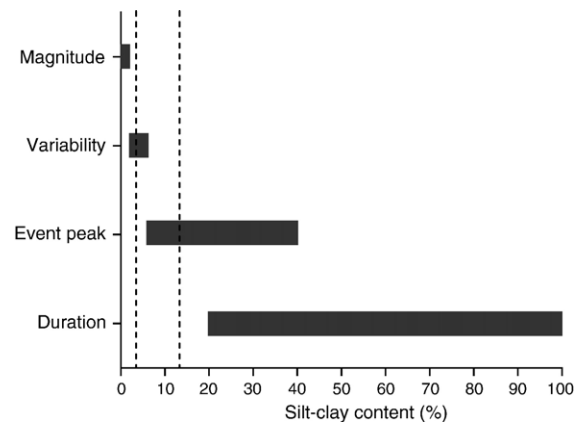


Fig. 8. Conceptual model of best predictors for erosion rates of cohesive riverbanks. The vertical dashed lines represent the range of bank silt–clay content used in this study.

ligible when compared to that caused by subaerial processes. For channel banks with silt–clay contents of 20–40%, both subaerial and hydraulic processes are possible agents of erosion, and their respective dominance can be spatially and temporally variable. Erosion of channel banks with <20% silt–clay is dominated by hydraulic shear. In these well-drained banks, subaerial erosion is insignificant compared to hydraulic erosion. For moderate silt–clay contents (6–20%), event peak of τ_{ex} is the best predictor of bank erosion rates. Thus, the maximum intensity of a flow event will dictate the amount of erosion. For banks with low silt–clay contents (2–6%), variability (i.e., all peaks) of τ_{ex} is the best predictor of bank erosion rates due to the susceptibility of low-resistance banks to all peak intensities. Channel banks with <2% silt–clay are considered to be noncohesive and, thus, magnitude of τ_{ex} dictates the amount of erosion. Because of the limited data set available for this conceptual model, the above nominal values for silt–clay content are only best estimates. Further, this conceptual model is susceptible to deviations where external factors affect the force–resistance relationship within the channel. Some examples already mentioned are vegetation and water-table elevations. In order to verify this model, the following would be needed: more accurate estimates of cohesive τ_c , a more accurate method to calculate τ_{bank} in natural channels, and future research on different channel types in a variety of environments.

We use this conceptual model (Fig. 8) to address the current model used for hydraulic erosion of cohesive riverbanks (Eq. (1)). The regression plots for *magnitude*, *event peak*, and *variability* (Fig. 7) substantiate the use of an erodibility coefficient (*k*). As the erodibility of bank material increased (i.e., τ_c de-

creased), the slope of the regression line (erosion rate) increased. The results of this study (Fig. 6) and those of Arulanandan et al. (1980) show that k increases exponentially with decreasing soil resistance. As for the model's calculation of τ_{ex} , this study showed that the amount of hydraulic erosion was not strongly correlated to the magnitude of τ_{ex} . For channel banks with moderate τ_c , the event peak of τ_{ex} (Fig. 5) best predicted erosion rates. For channel banks with low τ_c , the variability of τ_{ex} (Fig. 5) best predicted erosion rates. The current model used for hydraulic erosion of cohesive riverbanks (Eq. (1)) should be further researched with these concepts in mind.

6. Conclusions

Process dominance in cohesive bank erosion has been a problem for geomorphologists because of the complexity of electrochemical bonds within and between aggregates, and because of the multitude of interdependent variables operating on various spatial and temporal scales (see Lane and Richards, 1997). These impediments have led some researchers to conclude that the amount of cohesive bank erosion is “controlled by a complex combination of conditions and that no single model emerges” (Hooke, 1979, p. 60). In this study, we were able to remove the many factors that confound bank erosion analyses and evaluate hydraulic erosion as an independent process. Based on erosion measurements and excess shear stress estimates along transects in Sand River, we found that event peak of excess shear stress is the best predictor of bank erosion for moderately cohesive banks and variability of excess shear stress is the best predictor for minimally cohesive banks. These observations lead us to conclude that hydraulic bank erosion is dictated by flow peak intensities.

The results of this study are important to two applications. First, the accuracy of channel evolution models will depend on how accurate bank erosion is quantified. These models also need to be able to incorporate temporal variability in flow regime and channel form (see Benda et al., 2002). Second, a better comprehension of the controls on cohesive bank erosion will help stream managers to design drainage networks and restoration plans that will minimize bank erosion. For a given bank material, the manager can minimize the flow property that dictates erosion, as opposed to just lining the channel with riprap. In addition to these applications, this research has introduced results that can be used as a foundation for further research in critical shear stress values, excess shear stress distributions, and cohesive bank erosion processes.

Acknowledgements

This research was supported by NSF award EAR-9985345 to Torres. Also, the Hitchcock Foundation provided partial funding, access to the site, and technical support. This research benefited from the suggestions of William L. Graf, James H. Knapp, and Michael E. Meadows. Additionally, we are grateful for the assistance provided by numerous faculty, staff, and students from the Departments of Geology, Geography, and Civil and Environmental Engineering at the University of South Carolina. Martin W. Doyle and two anonymous reviewers provided comments that improved content and clarity of the manuscript.

References

- Arulanandan, K., Gillogley, E., Tully, R., 1980. Development of a quantitative method to predict critical shear stress and rate of erosion of natural undisturbed cohesive soils. USACE, Waterways Experiment Station Technical Report GL-80-5, Vicksburg, MS.
- ASCE Task Committee on Erosion of Cohesive Materials Erosion of cohesive sediments, 1968. *Journal of the Hydraulics Division*, ASCE 94 (HY4), 1017–1047.
- ASCE Task Committee on Hydraulics, Bank Mechanics, and Modeling of River Width Adjustment, 1998. River width adjustment: I. Processes and mechanisms. *Journal of Hydraulic Engineering* 124, 881–902.
- Babaeyan-Koopaei, K., Ervine, D.A., Carling, P.A., Cao, Z., 2002. Velocity and turbulence measurements for two overbank flow events in River Severn. *Journal of Hydraulic Engineering* 128 (10), 891–900.
- Benda, L.E., Poff, N.L., Tague, C., Palmer, M.A., Pizzuto, J., Cooper, S., Stanley, E., Moglen, G., 2002. How to avoid train wrecks when using science in environmental problem solving. *BioScience* 52 (12), 1127–1136.
- Beven, K., 1981. The effect of ordering on the geomorphic effectiveness of hydrologic events. *IAHS* 132, 510–526.
- Buffington, J.M., Montgomery, D.R., 1997. A systematic analysis of eight decades of incipient motion studies, with special reference to gravel-bedded rivers. *Water Resources Research* 33 (8), 1993–2029.
- Casagli, N., Rinaldi, M., Gargini, A., Curini, A., 1999. Pore water pressure and streambank stability: results from a monitoring site on the Sieve River, Italy. *Earth Surface Processes and Landforms* 24, 1095–1114.
- Chang, H.H., 1988. *Fluvial Processes in River Engineering*. Wiley and Sons, New York. 432 pp.
- Chow, V.T., 1959. *Open-Channel Hydraulics*. McGraw-Hill, New York. 680 pp.
- Conover, W.J., 1999. *Practical Nonparametric Statistics*. Wiley and Sons, New York. 584 pp.
- Couper, P., 2003. Effects of silt-clay content on the susceptibility of river banks to subaerial erosion. *Geomorphology* 56, 95–108.
- Cowan, W.L., 1956. Estimating hydraulic roughness coefficients. *Journal of Agricultural Engineering* 37 (7), 473–475.
- Darby, S.E., Thorne, C.R., 1996. Numerical simulation of widening and bed deformation of straight sand-bed rivers: I. Model development. *Journal of Hydraulic Research* 122 (4), 184–193.

- Draper, N.R., Smith, H., 1998. *Applied Regression Analysis*. Wiley and Sons, New York. 706 pp.
- Dunn, I.S., 1959. Tractive resistance of cohesive channels. *Journal of the Soil Mechanics and Foundations Division, ASCE* 85 (SM 3), 1–24.
- Flintham, T.P., Carling, P.A., 1988. The prediction of mean bed and wall boundary shear in uniform and compositely rough channels. In: White, W.R. (Ed.), *International Conference on River Regime*. Wiley and Sons, Chichester, UK, pp. 267–287.
- Gaskin, S.J., Pieterse, J., Al Shafie, A., Lepage, S., 2003. Erosion of undisturbed clay samples from the banks of the St. Lawrence River. *Canadian Journal of Civil Engineering* 30, 585–595.
- Gatto, L.W., 1995. Soil freeze–thaw effects on bank erodibility and stability. USACE, Cold Regions Research and Engineering Laboratory, Special Report 95-24, Hanover, NH.
- Grissinger, E.H., 1982. Bank erosion of cohesive materials. In: Hey, R.D., Thorne, C.R., Bathurst, J.C. (Eds.), *Gravel-bed Rivers*. Wiley and Sons, Chichester, UK, pp. 273–287.
- Grissinger, E.H., Little, W.C., Murphey, J.B., 1981. Erodibility of streambank materials of low cohesion. *Transactions of the ASAE*, 624–630.
- Hooke, J.M., 1979. An analysis of the processes of river bank erosion. *Journal of Hydrology* 42, 39–62.
- Huang, H.Q., Nanson, G.C., 1998. The influence of bank strength on channel geometry: an integrated analysis of some observations. *Earth Surface Processes and Landforms* 23, 865–876.
- Huang, H.Q., Warner, R.F., 1995. The multivariate controls of hydraulic geometry: a casual investigation in terms of boundary shear distribution. *Earth Surface Processes and Landforms* 20, 115–130.
- Khodashenas, S.R., Paquier, A., 1999. A geometrical method for computing the distribution of boundary shear stress across irregular straight open channels. *Journal of Hydraulic Research* 37 (3), 381–388.
- Knighton, A.D., 1973. Riverbank erosion in relation to streamflow conditions, River Bollin-Dean, Cheshire. *East Midland Geographer* 6, 416–426.
- Kondolf, G.M., 1997. Hungry water: effects of dams and gravel mining on river channels. *Environmental Management* 21 (4), 533–551.
- Lane, S.N., Richards, K.S., 1997. Linking river channel form and process: time, space and causality revisited. *Earth Surface Processes and Landforms* 22, 249–260.
- Langendoen, E.J., Simon, A., 2000. Stream Channel Evolution of Little Salt Creek and North Branch West Papillion Creek, Eastern Nebraska. USDA Report, ARS. National Sedimentation Laboratory, Oxford, MS.
- Lawler, D.M., 1986. River bank erosion and the influence of frost: a statistical examination. *Transactions of the Institute of British Geographers New Series* 11, 227–242.
- Lawler, D.M., 1993. Needle ice processes and sediment mobilization on river banks: the River Ilston, West Glamorgan, UK. *Journal of Hydrology* 150, 81–114.
- Le Bissonais, Y., 1996. Aggregate stability and assessment of soil crustability and erodibility: I. Theory and methodology. *European Journal of Soil Science* 47, 425–437.
- Millar, R.G., Quick, M.C., 1998. Stable width and depth of gravel-bed rivers with cohesive banks. *Journal of Hydraulic Engineering* 124 (10), 1005–1013.
- Newson, M.D., 1980. The geomorphological effectiveness of floods—a contribution stimulated by two recent events in mid-Wales. *Earth Surface Processes* 5, 1–16.
- Nystrom Jr., P.G., Willoughby, R.H., Kite, L.E., 1991. Cretaceous and Tertiary stratigraphy of the Upper Coastal Plain, SC. In: Horton Jr., J.W., Zullo, V.A. (Eds.), *The Geology of the Carolinas*. Univ. of Tennessee Press, Knoxville, pp. 221–240.
- Osman, A.M., Thorne, C.R., 1988. Riverbank stability analysis: I. Theory. *Journal of Hydraulic Engineering* 114 (2), 134–150.
- Osterkamp, W.R., Hedman, E.R., 1977. Variation of width and discharge for natural high-gradient stream channels. *Water Resources Research* 13 (2), 256–258.
- Papanicolau, A.N., 2001. Erosion of cohesive streambeds and banks. Report WRR-08, State of Washington Water Research Center. Washington State Univ, Pullman.
- Prosser, I.P., Hughes, A.O., Rutherford, I.D., 2000. Bank erosion of an incised upland channel by subaerial processes: Tasmania, Australia. *Earth Surface Processes and Landforms* 25, 1085–1101.
- Rhoads, B.L., Miller, M.V., 1991. Impact of flow variability on the morphology of a low-energy meandering river. *Earth Surface Processes and Landforms* 16, 357–367.
- Rinaldi, M., Casagli, N., 1999. Stability of streambanks in partially saturated soils and effects of negative pore water pressures: the Sieve River. *Geomorphology* 26, 253–277.
- Schumm, S.A., Harvey, M.D., Watson, C.C., 1984. *Incised Channels: Morphology, Dynamics and Control*. Water Resources Publications, Littleton, CO. 200 pp.
- Shields, I.A., 1936. Application of similarity principles and turbulence research to bed-load movement. In: Ott, W.P., van Uchelen, J.C. (Eds.), (Translators), *Hydrodynamics Laboratory Publication*, vol. 167. California Institute of Technology, Pasadena.
- Simon, A., 1992. Energy, time, and channel evolution in catastrophically disturbed fluvial systems. *Geomorphology* 5, 345–372.
- Simon, A., Collison, A.J.C., 2001. Pore-water pressure effects on the detachment of cohesive streambeds: seepage forces and matrix suction. *Earth Surface Processes and Landforms* 26, 1421–1442.
- Simon, A., Curini, A., Darby, S.E., Langendoen, E.J., 2000. Bank and near-bank processes in an incised channel. *Geomorphology* 35, 193–217.
- Simon, A., Langendoen, E.J., Thomas, R., 2003. Incorporating Bank-toe Erosion by Hydraulic Shear into a Bank-stability Model: Missouri River, Eastern Montana. First Interagency Conference on Research in the Watersheds. USDA ARS, Benson, AZ, pp. 70–76.
- Southeast Regional Climate Center (SERCC), 2004. Aiken, SC climate record. Aiken 4 NE, 1948–2004.
- Thorne, C.R., 1982. Processes and mechanisms of river bank erosion. In: Hey, R.D., Thorne, C.R., Bathurst, J.C. (Eds.), *Gravel-bed Rivers*. Wiley and Sons, Chichester, UK, pp. 227–259.
- Thorne, C.R., 1990. Effects of vegetation on river-bank erosion and stability. In: Thomes, J.B. (Ed.), *Vegetation and Erosion*. Wiley and Sons, Chichester, U.K., pp. 203–233.
- Twidale, C.R., 1964. Erosion of an alluvial bank at Birdwood, South Australia. *Zeitschrift für Geomorphologie* 8, 189–211.
- Vanoni, V.A. (Ed.), 1977. *Sedimentation Engineering*. ASCE, New York. 745 pp.
- Walker, H.J., Amborg, L., 1966. Permafrost and ice-wedge effect on river bank erosion. *Proceedings of the International Conference on Permafrost Washington, D.C.*, pp. 164–171.
- Wolman, M.G., 1959. Factors influencing erosion of a cohesive river bank. *American Journal of Science* 257, 204–216.